Fabrication of large-area ultra-thin single crystal silicon membranes

Z. Y. Dang,[1] M. Motapothula,[1] Y. S. Ow,[1] T. Venkatesan,[2] M. B. H. Breese,[1,3,a)] M. A. Rana,[4] and A. Osman[5]

[1]Center for Ion Beam Applications, Physics Department, National University of Singapore, Lower Kent Ridge Road, Singapore 117542, Singapore
[2]NanoCore, National University of Singapore, Singapore 117576, Singapore
[3]Singapore Synchrotron Light Source (SSLS), National University of Singapore, 5 Research Link, Singapore 117603, Singapore
[4]Physics Division, Directorate of Science, PINSTECH, P.O. Nilore, Islamabad, Pakistan
[5]National Centre for Physics (NCP), Shahdara Valley Road, Islamabad, Pakistan

Perfectly, crystalline, 55 nm thick silicon membranes have been fabricated over several square millimeters and used to observe transmission ion channeling patterns showing the early evolution of the axially channeled beam angular distribution for small tilts away from the [011] axis. The reduced multiple scattering through such thin layers allows fine angular structure produced by the highly non-equilibrium transverse momentum distribution of the channeled beam during its initial propagation in the crystal to be resolved. The membrane crystallinity and flatness were measured by using proton channeling measurements and the surface roughness of 0.4 nm using atomic force microscopy. © 2011 American Institute of Physics. [doi:10.1063/1.3665620]

Large-area, ultra-thin, free-standing silicon membranes are needed for diverse applications in ultraviolet, x-ray spectrometry, nano-electro-mechanical systems, sensors, and transmission ion channeling. Free-standing silicon membranes with nanometer thicknesses have been prepared and are discussed in Ref. [1]. However, their high curvature renders them unusable for ion channeling experiments, for which membranes need to be flat over areas of at least tens of micrometers. There are many approaches to fabricate thin, self-supporting silicon membranes over large areas, including introduction of a buried etch stop by diffusion or implantation[2] or a buried oxide[3] and electrochemical methods.[4,5] Cheung[6] developed the use of boron diffusion into silicon as an etch stop for ethylenediamine-pyrocatechol (EDP), allowing fabrication of such membranes over large areas. Such membranes were used for ion channeling studies in thin crystals[7–9] but they cannot be made much thinner than 200 nm with this process, and so the resultant channeling patterns are always blurred due to the significant amount of multiple scattering of the channeled trajectories. Ultra-thin silicon-germanium membranes were fabricated over micrometer areas,[10] but are too small for producing ion channeling patterns.

Ion channelling occurs when the transverse energy of an incident ion is less than the continuum potential energy of an atomic row or plane in a single crystal. Axial and planar ion channelling effects are important across a wide energy spectrum[11,12] from keV energies for ion implantation, MeV energies for ion beam analysis,[13,14] and GeV to TeV energies for proton beam extraction experiments.[15,16] A study of the angular distributions produced by MeV protons at small [011] axial tilts in silicon crystals of 200 to 300 nm thickness reported ring-like "doughnuts," concentric with [011] with a diameter proportional to the tilt and an azimuthal intensity which was modulated by the intersecting major planes.[17]

More recently, axial channelling in thin membranes was studied to characterise the effects of "rainbow" channelling[18,19] which predicts a singular differential transmission cross-section and the formation of fine structure such as points and ridges of width about 2% of the critical angle, ψ_a in the angular distribution through ultra-thin crystals. However, lack of perfectly crystalline, flat membranes thinner than 200 nm has hampered such experimental study of ion channeling in highly non-equilibrium conditions.

Here, we describe a method of fabricating ultra-thin silicon membranes over areas of 0.5 mm^2 based on potassium hydroxide (KOH) etching. This is usually performed in conjunction with a hard mask such as silicon nitride and silicon dioxide but problems of mechanical stresses and a finite etch rate hamper the use of such hard masks for producing ultra-thin membranes. Such problems recently led to the development of polymeric masking materials owing to their lower mechanical stresses.[20,21] Our method uses the buried oxide in a silicon-on-insulator (SOI) wafer as an etch stop for KOH etching through a back-side opening in a protective polymer layer. The SOI wafer comprises a 55 nm thick device layer (1 Ω cm, p-type), a 145 nm buried oxide and a substrate of 700 μm thickness. To etch through such a thick substrate, the wafer is immersed in KOH for many hours, necessitating a very high resistance polymer mask. We used ProTEK® B3 Wet-Etch Protective Coatings (Brewer Science) which exhibited excellent durability in a KOH concentration of 20% (in de-ionized water with 4% isopropyl alcohol) during extended etching times at 85 °C, achieving an etch rate of 100 μm/h. While the roughness of a silicon surface which is deeply etched with KOH is high, the buried oxide stops etching at regions which are more rapidly etched, allowing the slower-etched regions to fully remove the remaining substrate before any penetration of the oxide occurs. Since KOH provided sufficient Si:SiO$_2$ etching selectivity by a factor of at least one thousand,[22] higher selectivity but more hazardous etchants such as tetramethylammonium

a)Author to whom correspondence should be addressed. Electronic mail: phymbhb@nus.edu.sg.
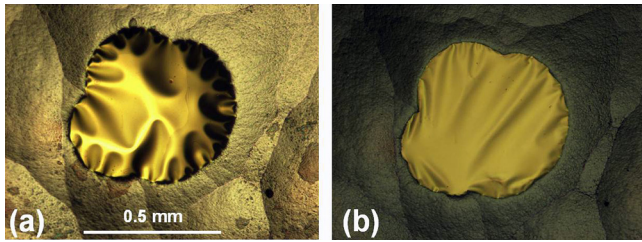
FIG. 1. (Color online) Optical micrographs of the same 55 nm silicon membrane (a) before and (b) after oxide removal.

hydroxide or EDP are not required. After etching, the polymer coating was removed from all surfaces using a Piranha. Finally, the SiO_2 layer is removed by dipping sample in dilute hydrofluoric acid (2%). A critical issue at this point is whether the ultra-thin membrane can withstand strain induced by the oxide layer without rupturing. While the membrane in Fig. 1(a) is clearly buckled before removal of the oxide, after removal, the membrane is much flatter, Fig. 1(b), and the lower surface exposed.

To study the crystalline quality of the free-standing membranes, we performed ion channeling analysis in conjunction with Rutherford backscattering spectrometry (RBS). No subsequent steps were taken to remove any native oxide from either exposed membrane surface before loading into a vacuum chamber for measurements at a chamber pressure of about 5×10^{-5} mbar. Figure 2(a) shows random and channeled backscattering spectra from the membrane, recorded at a scattering angle of 160° using a surface barrier detector resolution of about 12 keV. Simulation of the random spectrum confirms a thickness of 55 nm, which is calculated to contribute a full width at half maximum (FWHM) angular spread of only 0.01° for a 2 MeV proton beam due to multiple scattering. For axial channeling critical angles of about 0.20° for 2 MeV protons in the silicon major axes, this represents an angular spread of ~5% of the critical angle, allowing finer angular structure to be observed than was previously possible with thicker membranes. The RBS minimum scattering yield in channeled compared to random alignment is 5.5%, confirming the highly crystalline nature of the membrane. The root-mean-square roughness of the back surface of 10 μm thick membrane prepared using the same process (the 55 nm membranes are very fragile) was measured by atomic force microscopy as 0.4 nm, comparable with a virgin surface.

Figure 2(b) shows the bend angle across a 55 nm membrane, measured by observing the change in angular location of the [011] axis in a channeling pattern produced by a focused 2 MeV proton beam. The membrane is reasonably flat across the central region but typically varies by 0.05° for a 25 μm lateral distance. Use of a broad, unfocused proton beam size of only 100 μm would still encompass a large range of bends which would severely limit observation of any fine angular structure in the channeling patterns. An important advance here is the use of a nuclear microprobe[23] in
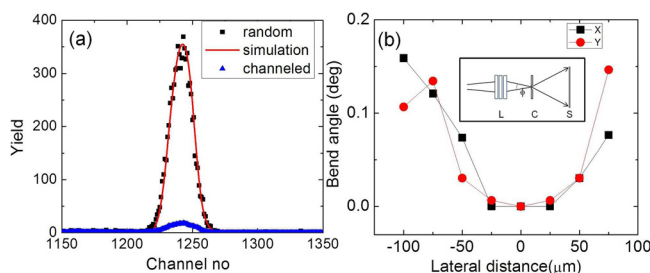

FIG. 2. (Color online) (a) RBS random and [001] channeling spectra of a 55 nm membrane using 2 MeV protons for a charge of 20 nC in both cases. A simulation of a 55 nm silicon layer in random alignment is also shown. (b) Measured magnitude of bend angle across a membrane surface in orthogonal directions. The inset shows a schematic of nuclear microprobe lens system (**L**) to focus the beam on the crystal membrane with the channeling pattern observed on a fluorescent screen (**S**) 50 cm further downstream.
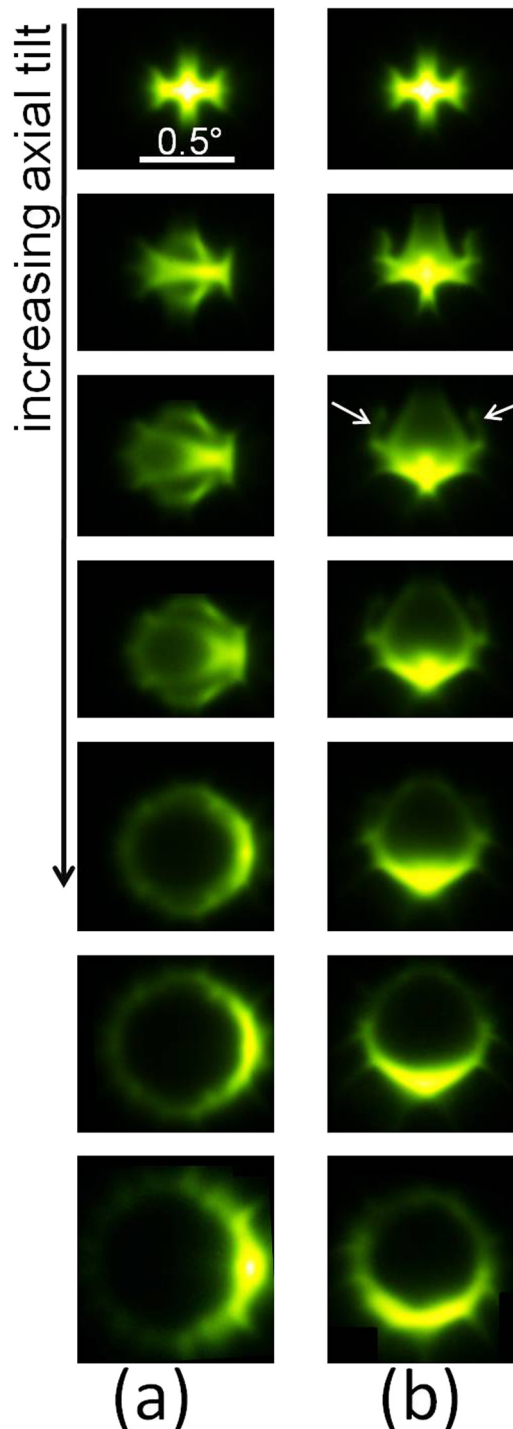

FIG. 3. (Color online) Experimental channeling patterns recorded for 2 MeV protons from a 55 nm [001] Si membrane for increasing tilts away from the [011] axis, in increments of $\psi_a/6$. The tilt planes are: (a) horizontally running (100) and (b) vertically running ($1\bar{1}0$).

which MeV ion beams can be focused to less than 1 μm on the wafer surface, so any gradual bend does not limit the resolvable angular structure in the channeling patterns.

Figure 3 shows experimental channeling patterns for 2 MeV protons transmitted through a 55 nm thick [001] silicon membrane around the [011] axis within the (a) horizontally running (001) plane and (b) vertically running ($1\bar{1}0$) plane. The patterns were recorded by photographing a highly sensitive aluminium-coated YAG scintillator screen 50 cm downstream of the membrane, using a beam current of about 10 pA with a beam convergence angle of $\sim$0.01°, and a camera exposure time of 0.8 s.

Figure 4 shows FLUX (Refs. 24 and 25) simulations of the exit angular distribution of forty thousand 2 MeV protons transmitted through silicon membranes for increasing tilt away from the [011] axis under the same conditions as in Fig. 3. FLUX uses the Ziegler-Biersack-Littmark universal

potential and a binary collision model with an impact parameter dependent algorithm for energy loss. In Figs. 3 and 4, the top of each column shows the pattern at axial alignment and the bottom of each column shows the pattern at a tilt equal to the axial channeling critical angle, ψ_a. Columns (a) and (b) of these two figures provide a comparison of experimental and simulated patterns through ultra-thin membranes. The layer thicknesses in Fig. 4 are based on the experimental geometry where the 55 nm thick [001] membrane is tilted through 45° to the [011] axis, giving a longer path length through the crystal. Fig. 4(c) shows simulated patterns for a thicker membrane so that the effect of multiple scattering in obscuring the fine angular structure observed in thinner membranes is demonstrated. The most distinctive feature of the [011] patterns in Fig. 3 for tilting along the horizontally running (001) direction is the formation of a double ring-like structure and on tilting along the vertically running ($1\bar{1}0$) direction is the formation of an half an elongated hexagon with separated outer arms (arrowed). These features are both well-reproduced in the [011] simulated patterns in Fig. 4 and are obscured in the simulated patterns through a thicker layer. While these features have been predicted in simulations,[26] they have never been previously observed.
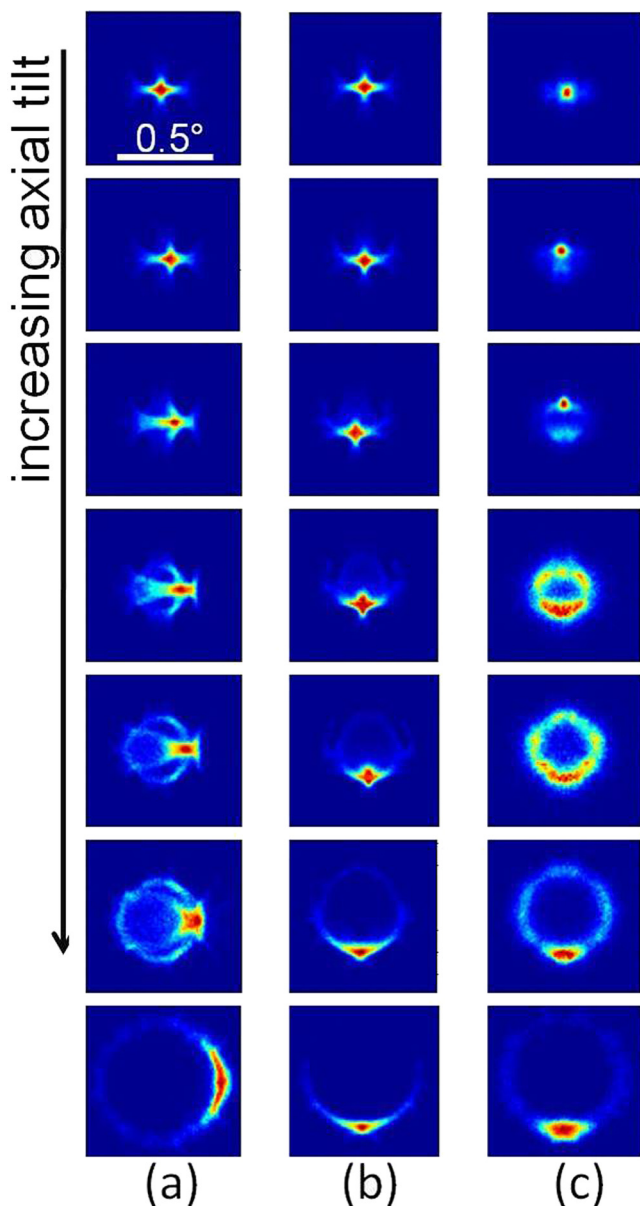

FIG. 4. (Color online) Flux simulations for the angular distributions of 2 MeV protons transmitted through a silicon [011] membrane for increasing tilt away from the axis in increments of $\psi_a/6$. The membrane thickness and tilt planes are: (a) 80 nm (100), (b) 80 nm ($1\bar{1}0$), and (c) 300 nm (110).

[1]J. A. Rogers, M. G. Lagally, and R. G. Nuzzo, Nature **477**, 45 (2011).
[2]S. D. Collins, J. Electrochem. Soc. **144**, 2242 (1997).
[3]C. Constancias, B. Dalzotto, P. Michallon, J. Wallace, and M. Saib, J. Vac. Sci. Technol. B **28**, 194 (2010).
[4]B. K. Ju and M. H. Oh, J. Mater. Sci. **29**, 664 (1994).
[5]A. Ogura, Jpn. J. Appl. Phys. Part 2 **35**, L71 (1996).
[6]N. W. Cheung, Rev. Sci. Instrum. **51**, 1212 (1980).
[7]J. S. Rosner, W. M. Gibson, J. A. Golovchenko, A. N. Goland, and H. E. Wegner, Phys. Rev. B **18**, 1066 (1978).
[8]H. F. Krause, J. H. Barrett, S. Datz, P. F. Dittner, N. L. Jones, J. Gomez del Campo, and C. R. Vane, Phys. Rev. A **49**, 283 (1994).
[9]M. B. H. Breese, P. J. C. King, G. W. Grime, P. J. M. Smulders, L. E. Seiberling, and M. A. Boshart, Phys. Rev. B **53**, 8267 (1996).
[10]M. M. Roberts, L. J. Klein, D. E. Savage, K. A. Slinker, M. Friesen, G. Celler, M. A. Eriksson, and M. G. Lagally, Nature Mater. **5**, 388 (2006).
[11]*Channeling, Theory, Observation and Applications*, edited by D. V. Morgan (Wiley, London, 1973).
[12]D. Gemmell, Rev. Mod. Phys. **46**, 129 (1974).
[13]L. C. Feldman, J. W. Mayer, and S. T. Picraux, *Materials Analysis by Ion Channeling* (Academic, New York, 1982).
[14]M. B. H. Breese, P. J. C. King, P. J. M. Smulders, and G. W. Grime, Phys. Rev. B **51**, 2742 (1995).
[15]V. M. Biryukov, Yu. A. Chesnokov, and V. I. Kotov, *Crystal Channeling and its Application at High Energy Accelerators* (Springer, Berlin, 1997).
[16]R. A. Carrigan, Jr., D. Chen, G. Jackson, N. Mokhov, C. T. Murphy, S. I. Baker, S. A. Bogacz, D. Cline, S. Ramachandran, J. Rhoades *et al.*, Phys. Rev. ST Accel. Beams **1**, 022801 (1998).
[17]J. S. Rosner, W. M. Gibson, J.A. Golovchenko, A. N. Goland, and H. E. Wegner, Phys. Rev. B **18**, 1066 (1978).
[18]N. Nešković, Phys. Rev. B **33**, 6030 (1986).
[19]H. F. Krause, J. H. Barrett, S. Datz, P. F. Dittner, N. L. Jones, J. Gomez del Campo, and C. R. Vane, Phys. Rev. A **49**, 283 (1994).
[20]K. Ruben, T. Flaim, and C. Li, Proc. SPIE **5342**, 212 (2004).
[21]G. Canavese, S. L. Marasso, M. Quaglio, M. Cocuzza, C. Ricciardi, and C. F. Pirri, J. Micromech. Microeng. **17**, 1387 (2007).
[22]K. E. Bean, IEEE Trans. Electron Devices, **25**, 1185 (1978).
[23]M. B. H. Breese, E. J. Teo, M. A. Rana, L. Huang, J. A. van Kan, F. Watt, and P. J. C. King, Phys. Rev. Lett. **92**, 045503 (2004).
[24]P. J. M. Smulders and D. O. Boerma, Nucl. Instrum. Methods Phys. Res. B **29**, 471 (1987).
[25]P. J. M. Smulders, D. O. Boerma, and M. Shaanan, Nucl. Instrum. Methods Phys. Res. B **45**, 450 (1990).
[26]D. Borka, S. Petrovic, and N. Neskovic, J. Electron Spectrosc. Relat. Phenom. **129**, 183 (2003).